Electronic structure of the Si(111)-$\sqrt{21}\times\sqrt{21}$-(Ag+Au) surface

Xiao Tong*
Core Research for Evolutional Science and Technology, The Japan Science and Technology Corporation, Kawaguchi Center Building, Hon-cho 4-1-8, Kawaguchi, Saitama 332, Japan

Chun Sheng Jiang† and Shuji Hasegawa‡
Department of Physics, School of Science, University of Tokyo, 7-3-1 Hongo, Bunkyo-ku, Tokyo 113, Japan
(Received 1 May 1997; revised manuscript received 17 July 1997)

Angle-resolved ultraviolet and x-ray photoelectron spectroscopies were used to analyze the electronic band structure of the Si(111)-$\sqrt{21}\times\sqrt{21}(R\pm10.89°)$-(Ag+Au) surface that was induced by Au adsorption of 0.19 atomic layer onto the Si(111)-$\sqrt{3}\times\sqrt{3}$-Ag surface at room temperature. We found two intrinsic dispersive surface-state bands crossing the Fermi level, which were considered to originate from an antibonding surface state of the initial $\sqrt{3}\times\sqrt{3}$-Ag structure. The electrons accumulated in these bands were found to be donated by Au adatoms. The electron transfer from Au adatoms into the substrate bulk (surface space-charge layer) was also confirmed by measuring the changes in band bending. The results seemed to be consistent with an atomic model in which the Au adatoms sit atop the Ag trimers of the $\sqrt{3}\times\sqrt{3}$-Ag framework. We proposed a kind of atomic bonding mechanism on this surface, referred to as ''parasitic surface bonding,'' where Au adatoms make metallic bonds via a surface-state band of the substrate surface. [S0163-1829(98)02515-6]

I. INTRODUCTION

Surface superstructures of a $\sqrt{21}\times\sqrt{21}(R\pm10.89°)$ periodicity are known to emerge by adsorption of a submonolayer noble metal (Au, Ag, or Cu) onto the Si(111)-$\sqrt{3}\times\sqrt{3}$-Ag surface.[1–5] These $\sqrt{21}\times\sqrt{21}$ superstructures exhibit some interesting common features, which have driven us into a series of investigations including the present study.[6–8]

First of all, from the point of view of atomic structures, the $\sqrt{21}\times\sqrt{21}$ surfaces seem to be formed only by periodic simple adsorption of the noble-metal adatoms on the $\sqrt{3}\times\sqrt{3}$-Ag framework. In fact, based on scanning tunneling microscopy (STM) observations, Nogami, Wan, and Lin[1] proposed a structural model for the $\sqrt{21}\times\sqrt{21}$ superstructure induced by Au adsorption [hereafter referred to as $\sqrt{21}\times\sqrt{21}$-(Ag+Au)]; Au adatoms should sit on the centers of some of the Ag trimers in the honeycomb-chained-trimer (HCT) structure[9] of the $\sqrt{3}\times\sqrt{3}$-Ag surface. The Au coverage should be 0.24 monolayer (MI) in their model. On the other hand, Ichimiya, Nomura, and Horio derived another structural model for the same surface based on STM and reflection high-energy electron diffraction (RHEED) observations.[2] Au adatoms should sit on the centers of some of the Si trimers of the HCT structure. Protrusions in STM images, in their conclusions, might be due to electronic states induced by Au adatoms and do not directly correspond to the adatoms. The Au coverage was 0.14 ML in their model. Both models, however, suggest a common feature that the HCT framework of the initial $\sqrt{3}\times\sqrt{3}$-Ag surface is not broken. So it can be expected that a rich knowledge on the atomic and electronic structures of the $\sqrt{3}\times\sqrt{3}$-Ag surface[10] will be useful to discuss those of the $\sqrt{21}\times\sqrt{21}$ superstructures.

The second point to be questioned is how noble-metal adatoms make bonds with the substrate. Since the $\sqrt{3}\times\sqrt{3}$-Ag surface is known to have no dangling bonds,[11–13] the answer for this question is not trivial. The electronic states for atom bondings should be clarified to determine the atomic structure.

The third point to be interested in is the electrical conductance parallel to the surface. In our previous papers,[6–8,14,15] we have reported a very high electrical conductance for all the $\sqrt{21}\times\sqrt{21}$ surfaces induced by Au, Ag, and Cu adsorptions. Photoemission spectroscopy measurements suggested that the high surface electrical conductances were not due to the surface space-charge layer but rather due to surface-state bands. In fact, dispersive surface-state bands crossing the Fermi level (E_F) were found on the $\sqrt{21}\times\sqrt{21}$-(Ag+Au) surface by our preliminary measurements of angle-resolved ultraviolet photoelectron spectroscopy (ARUPS).[7,8]

In the present paper, we thoroughly analyze the evolution of the electronic structures during the structural conversion from the $\sqrt{3}\times\sqrt{3}$-Ag to the $\sqrt{21}\times\sqrt{21}$-(Ag+Au) superstructures, in connection with their atomic structures. The results can be understood by some characteristic modulations of the atomic and electronic structures of the initial $\sqrt{3}\times\sqrt{3}$-Ag surface. So we will begin with the reanalysis of the electronic structure of the $\sqrt{3}\times\sqrt{3}$-Ag surface, comparing it with previous reports on it.[13,16,17] From our systematic investigations, we have proposed a kind of mechanism for surface-atom bonding, called parasitic surface bonding, where adsorbate atoms make metallic bonds with each other via a surface-state band of the substrate surface. The correlation between the surface electrical conductance and the electronic structure of the $\sqrt{21}\times\sqrt{21}$-(Ag+Au) surface will be discussed briefly and its details will be given elsewhere.

II. EXPERIMENT

Experiments were carried out in an ultrahigh vacuum apparatus whose base pressure was below 5×10^{-10} Torr. It

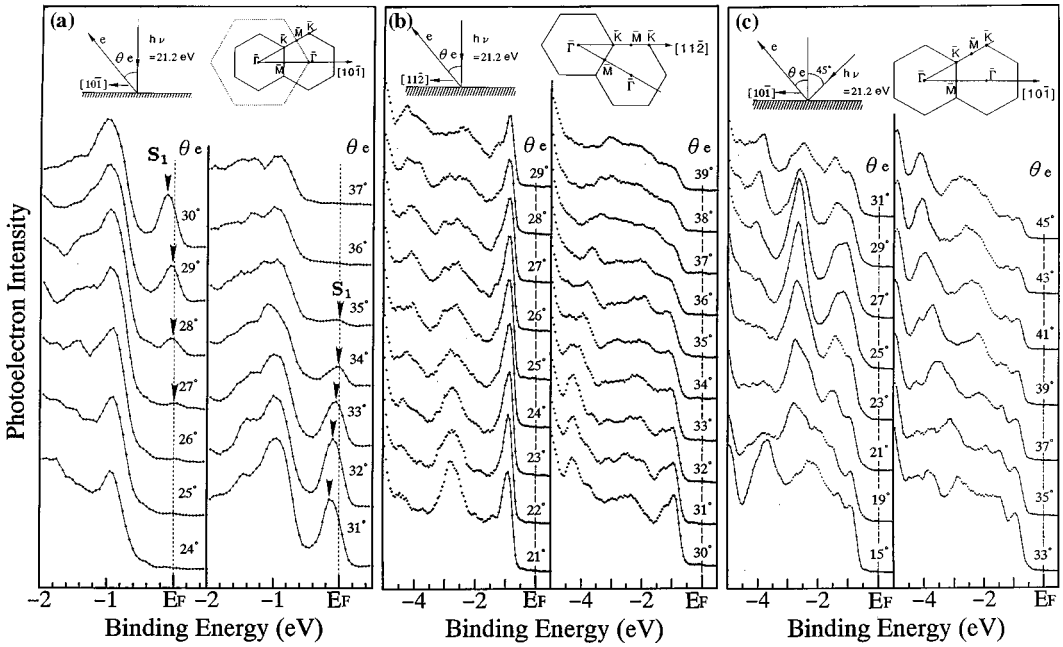

FIG. 1. ARUPS spectra taken from the Si(111)-$\sqrt{3}\times\sqrt{3}$-Ag surface at room temperature. The excitation light was He I with (a) and (b) normal incidence and (c) 45° from the surface normal. The electron emission angles θ_e were changed from the surface normal to (a) [101], (b) [11$\bar{2}$], and (c) [10$\bar{1}$] directions, respectively.

consisted of a RHEED system, an x-ray source, an ultraviolet (UV) light source, and an electron analyzer (VG ADES 500). The x-ray source for x-ray photoelectron spectroscopy (XPS) had a twin anode of Mg and Al. It produced a Mg $K\alpha$ (1253. 6 eV) or an Al $K\alpha$ (1486.6 eV) line. Their full widths at half maximum (FWHM's) were about 0.8 and 0.9 eV, respectively. The UV light source used in ultraviolet photoelectron spectroscopy (UPS) experiments was an unpolarized He I (21.22 eV) emission, whose energy width was about 4 meV, sufficiently small compared to the energy resolution of the electron energy analyzer. The energy of photoelectrons emitted from the sample surface was analyzed by a hemispherical electron analyzer that could rotate around two axes centering the sample. The angular resolution was about 2°, which was estimated from the prospecting angle of the entrance aperture of the analyzer from the sample. The typical energy resolution was 0.1 eV when the pass energy was set to 10.0 eV.

The substrate was a p-type Si(111) wafer of 20 Ω cm resistivity at room temperature (RT) and its typical dimension was $25\times4\times0.4\ \mathrm{mm}^3$. A clear 7×7 RHEED pattern was produced by flashing the sample at 1200 °C several times by direct current around 10 A through it. The $\sqrt{3}\times\sqrt{3}$-Ag structure was made at a substrate temperature of 450 °C by depositing Ag with a rate of 0.66 ML/min. After cooling the substrate down to RT, the $\sqrt{21}\times\sqrt{21}$-(Ag+Au) structure was formed by depositing Au of about 0.19 ML coverage onto the $\sqrt{3}\times\sqrt{3}$-Ag surface with a rate of 0.50 ML/min. The structural conversions were always monitored by RHEED during the depositions. The coverages of Ag and Au were calibrated using their deposition durations with constant deposition rates by assuming that 1 ML of Ag and 0.5 ML of Au are needed for complete conversions in RHEED patterns from the 7×7 structure to the $\sqrt{3}\times\sqrt{3}$-Ag (Refs. 9 and 18) and the 5×2-Au superstructures,[19] respectively.

III. RESULTS

A. ARUPS for the Si(111)-$\sqrt{3}\times\sqrt{3}$-Ag surface

Figure 1(a) shows the ARUPS spectra taken from the Si(111)-$\sqrt{3}\times\sqrt{3}$-Ag surface at RT with normal incidence of UV light. The photoelectron detection angles θ_e were changed from the surface normal in an orientation along [101]. The angles θ_e presented here correspond to the surface-parallel wave vector around the $\bar{\Gamma}$ point ($\theta_e\approx31°$) in the second $\sqrt{3}\times\sqrt{3}$ surface Brillouin zone (SBZ). The binding energy is referred to as E_F, which was determined from the metallic edge in an UPS spectrum from a Ta sample holder. A strong dispersive peak near E_F can be observed at the emission angles around $\theta_e=27°-35°$, as indicated by arrowheads. This is called the S_1 surface state band. Its bottom is located at about 0.18 eV below E_F. From these measurements, we have constructed a two-dimensional band-dispersion diagram shown in Fig. 2 (solid circles). This result is very similar to the report by Johansson *et al.*, although they used a heavily doped n^+-type Si crystal with polarized UV light from a synchrotron.[16] We have measured the spectra with the incident angles of UV light $\theta_i=0°$, 15°, 30°, 45°, and 60° measured from the surface normal. With $\theta_i=15°$, the S_1 peak was slightly weaker than at $\theta_i=0°$, but still observable. At $\theta_i=30°$ we could not obtain meaningful spectra around $\theta_e=30°$ because the reflection of the UV light was so strong around this angle (in our apparatus, the detection angle θ_e coincided with the specular reflection angle of the incident UV light at $\theta_i=\theta_e=30°$). Therefore, since the S_1 peak was observable, if it exists, only in the narrow range of angles around $\theta_e=30°$, we could not judge whether or not the S_1 peak was detectable at $\theta_i=30°$. However, we could definitely say that no peaks could be observed around E_F at any emission angles with $\theta_i=45°$ and 60°.

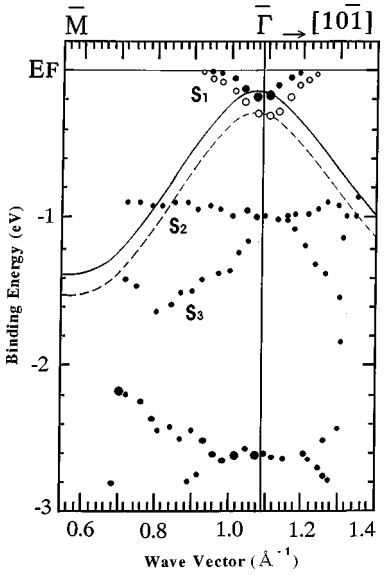

FIG. 2. Two-dimensional band-dispersion diagram for the Si(111)-$\sqrt{3}\times\sqrt{3}$-Ag surface. Closed circles indicate the peak position in the ARUPS of Fig. 1(a). Open circles are for the $\sqrt{3}\times\sqrt{3}$-Ag surface covered by 0.1 ML of Au (see Fig. 3). Their sizes qualitatively correspond to the intensity of the respective peaks. The symbols $\bar{\Gamma}$ and $\bar{M}$ are symmetric points in the $\sqrt{3}\times\sqrt{3}$ surface Brillouin zone. The solid curve represents the upper edge of the projected bulk valence band including band-bending effect at the initial $\sqrt{3}\times\sqrt{3}$-Ag surface. The broken curve is that for the $\sqrt{3}\times\sqrt{3}$-Ag surface covered by 0.1 ML of Au.

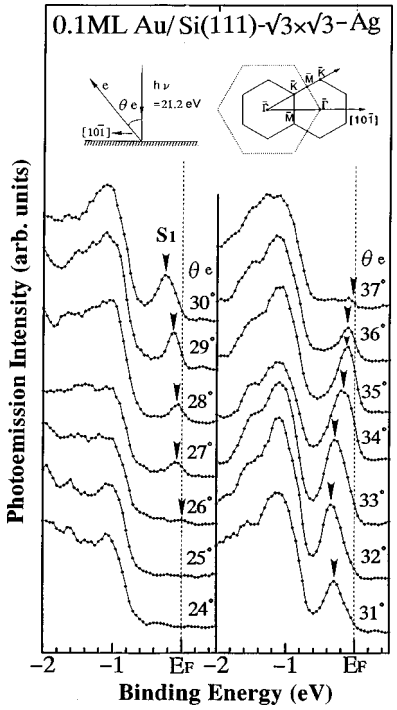

FIG. 3. ARUPS spectra taken from the $\sqrt{3}\times\sqrt{3}$-Ag surface, which was covered by 0.1 ML of Au. The excitation light was illuminated with normal incidence. The electron emission angles θ_e were changed from the surface normal to the [10$\bar{1}$] direction.

Figure 1(c) shows the spectra taken at $\theta_i=45°$ with the other conditions kept the same as in Fig. 1(a). There is no emission intensity around E_F at all emission angles used. This is consistent with the reports by Yokotsuka *et al.*[13] and Hansson *et al.*,[17] where the S_1 state is not detected at $\theta_i=45°$. In our previous paper,[7] we could not determine the S_1 band in ARUPS measurements either because the illumination angles θ_i were set again to be 30° or 45° from the surface normal. So we stated incorrectly in that paper that the bottom of the S_1 band should be located above E_F so that the S_1 band would be empty and that only the (conduction) electrons thermally excited from the filled states would exist (though this is a situation predicted by the first-principles calculations[11,12]). From the present studies, however, we have become aware that the S_1 band can be actually observed only when the UV illumination angle θ_i is set to be less than 15°. This point indicates that this surface electronic state is excited only by the component of electric vector of light parallel to the surface. This symmetry means that the S_1 state consists mainly of p_x and p_y components (the xy plane is on the surface). One might expect, however, that there should be a sufficient parallel electric-vector component to make the S_1 peak observable even at $\theta_i=45°$ or 60°. However, we could not detect it at these illumination angles. This means that the emission intensity is not simply proportional to the parallel electric-vector component of the light, suggesting some photoelectron diffraction effect.

In scanning the electron analyzer in the [11$\bar{2}$] direction, we could not detect any emission intensity near E_F even at $\theta_i=0°$, as shown in Fig. 1(b). This is because the $\bar{\Gamma}$ point does not exist in the [11$\bar{2}$] direction in the measured range of θ_e. The S_1 band appears only in a narrow range near $\bar{\Gamma}$ point in the $\sqrt{3}\times\sqrt{3}$ SBZ.

B. ARUPS for the Si(111)-$\sqrt{21}\times\sqrt{21}$-(Ag+Au) surface

When Au of about 0.1 ML coverage was deposited onto this $\sqrt{3}\times\sqrt{3}$-Ag surface at RT, the RHEED pattern still showed the same $\sqrt{3}\times\sqrt{3}$ pattern without any $\sqrt{21}\times\sqrt{21}$ superspots. However, the corresponding ARUPS changed as shown in Fig. 3. Compared to the spectra of the initial $\sqrt{3}\times\sqrt{3}$-Ag surface [Fig. 1(a)], the features scarcely changed, but the whole spectra shifted towards higher binding energy. In particular, the S_1 band shifted by approximately 0.16 eV and its intensity became stronger. The S_1 band at this surface is plotted by open circles in the dispersion diagram of Fig. 2.

When Au was further deposited onto the surface, the $\sqrt{21}\times\sqrt{21}$ superreflection spots began to appear in the RHEED pattern from about 0.13 ML coverage and the spots became the strongest around 0.19 ML coverage. Figure 4 shows the ARUPS spectra taken from the Si(111)-$\sqrt{21}\times\sqrt{21}$-(Ag+Au) surface with $\theta_i=0°$, scanned in the [101] direction. Two upward-dispersive peaks appear near E_F, as indicated by big and small arrowheads. Here we call them S_1^* and S_1' bands, respectively. The bottom of the S_1^* band is much lower than that of the S_1' band below E_F. When θ_i was set to be 30°, the emission peaks corresponding to the S_1' and S_1^* bands could be observed as shown in our previous paper,[7] but they were slightly weaker than at $\theta_i=0°$. The two peaks dispersed not only in a narrow range of θ_e around $\theta_e=30°$, but also in a wider range of angle, so that we could detect them in spite of strong reflection of UV light at θ_e

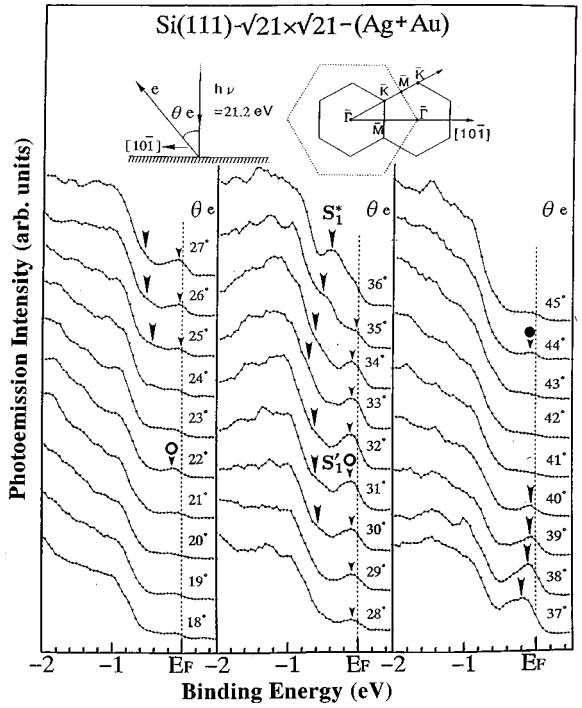

FIG. 4. ARUPS spectra taken from the $\sqrt{21}\times\sqrt{21}$-(Ag+Au) surface. The excitation light was illuminated with normal incidence. The electron emission angles θ_e were changed from the surface normal to the [101] direction. Open and closed circles marked at some of the small arrowheads correspond to the respective positions in the $\sqrt{21}\times\sqrt{21}$ surface Brillouin zone shown in Fig. 6.

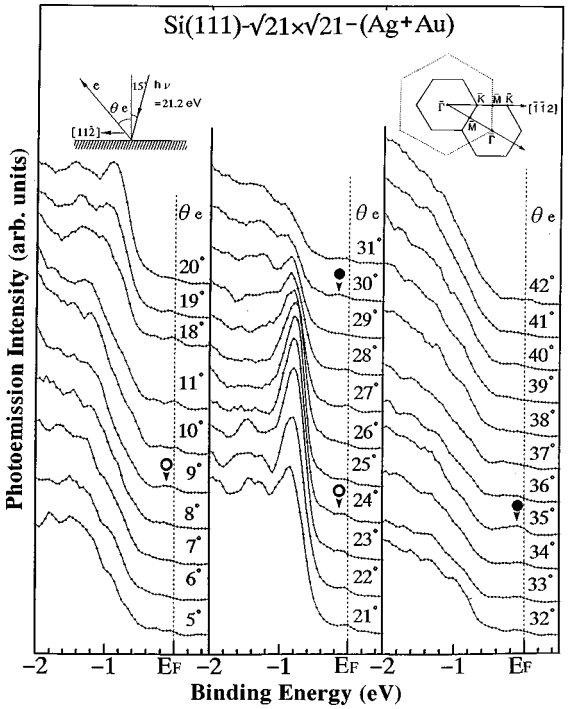

FIG. 5. ARUPS spectra taken from the $\sqrt{21}\times\sqrt{21}$-(Ag+Au) surface. The excitation light was illuminated in a direction 15° off the surface normal. The electron emission angles θ_e were changed from the surface normal to the [11$\bar{2}$] direction. Open and solid circles marked at some of the small arrowheads correspond to the respective positions in the $\sqrt{21}\times\sqrt{21}$ surface Brillouin zone shown in Fig. 6.

$=30°$. At $\theta_i=45°$, the S_1' and S_1^* peaks were very weak, but still recognizable (though the S_1 peak at the initial $\sqrt{3}\times\sqrt{3}$-Ag surface was not detectable at all with $\theta_i=45°$). This slight difference in illumination angles for detecting the surface-state peaks between the $\sqrt{21}\times\sqrt{21}$-(Ag+Au) phase and $\sqrt{3}\times\sqrt{3}$-Ag phase might mean a slight change in symmetry of wave functions of the electronic states or a change in the photoelectron diffraction effect. However, it still can be said that the S_1' and S_1^* states consist mainly of p_x and p_y components as in the case of the S_1 state of the initial $\sqrt{3}\times\sqrt{3}$-Ag surface.

We also measured the ARUPS from the same Si(111)-$\sqrt{21}\times\sqrt{21}$-(Ag+Au) surface scanned in the [11$\bar{2}$] direction and $\pm 10.89°$ off the [101] direction with $\theta_i=0°$, 15°, 30°, and 45°. For the initial $\sqrt{3}\times\sqrt{3}$-Ag surface, no emission near E_F could be observed in these directions [see Fig. 1(b)]. However, in the spectra from the $\sqrt{21}\times\sqrt{21}$-(Ag+Au) surface, weak peaks near E_F could be observed, but they were not so prominent compared to those in the [101] direction shown in Fig. 4. For example, Fig. 5 shows the ARUPS taken in the [11$\bar{2}$] direction with $\theta_i=15°$. We notice weak peaks around 0.15 eV below E_F, as indicated by small arrowheads. These were not observed at the initial $\sqrt{3}\times\sqrt{3}$-Ag surface [compare with Fig. 1(b)].

In Fig. 6 we show the SBZ's of the 1×1, $\sqrt{3}\times\sqrt{3}$, and $\sqrt{21}\times\sqrt{21}(R\pm10.89°)$ periodicities. Because the $\sqrt{21}\times\sqrt{21}$-(Ag+Au) surface has double equivalent domains rotated by $\pm10.89°$ from the [101] direction, respectively, we must consider two types of SBZ's for this structure as shown in Fig. 6. The symbols $\bar{\Gamma}$, $\bar{M}$, and $\bar{K}$ are symmetric points of the $\sqrt{3}\times\sqrt{3}$ SBZ. Here we show the points (and emission angles θ_e) corresponding to the wave vectors for the emission peaks indicated by some of the small arrowheads with open and closed circles in Figs. 4 and 5. We notice that the peaks indicated by open and closed circles in Figs. 4 and 5

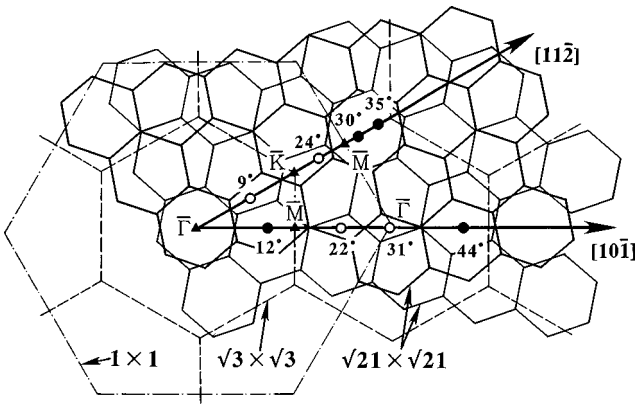

FIG. 6. The 1×1, $\sqrt{3}\times\sqrt{3}$, and $\sqrt{21}\times\sqrt{21}$ surface Brillouin zones (SBZ's) are represented by dot-dashed lines, dashed lines, and solid lines, respectively. The symbols $\bar{\Gamma}$, $\bar{K}$, and $\bar{M}$ are symmetric points in the $\sqrt{3}\times\sqrt{3}$ SBZ. The positions of the open and closed circles show the values of the wave vector $k_{\parallel}$ of photoelectrons (and the respective θ_e), which correspond to some of the small arrowheads with open and closed circles marked in Figs. 4 and 5. The open and closed circles imply the respective equivalent points in the $\sqrt{21}\times\sqrt{21}$ SBZ.

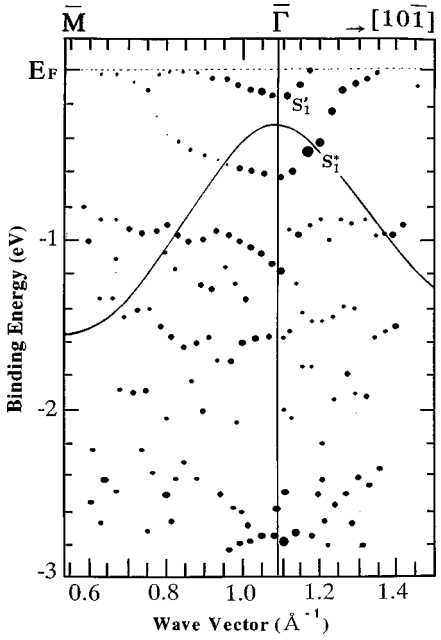

FIG. 7. Two-dimensional band-dispersion diagram for the $\sqrt{21}\times\sqrt{21}$-(Ag+Au) structure. Closed circles indicate the peak position in the ARUPS of Fig. 4. Their sizes qualitatively correspond to the intensity of the respective peaks. The symbols $\bar{\Gamma}$ and $\bar{M}$ are symmetric points in the $\sqrt{3}\times\sqrt{3}$ SBZ. The solid curve represents the upper edge of the projected bulk valence band including the band-bending effect.

correspond to the same positions, respectively, in the $\sqrt{21}\times\sqrt{21}$ SBZ as shown in Fig. 6. These points are respectively identical in the reduced SBZ. Therefore, we can conclude that these peaks do not originate from the surface-defects states but rather they are the peaks intrinsic in the $\sqrt{21}\times\sqrt{21}$ structure.

Figure 7 shows a two-dimensional band-dispersion diagram for the $\sqrt{21}\times\sqrt{21}$-(Ag+Au) surface, obtained from Fig. 4. The sizes of the solid circles qualitatively correspond to the intensity of the respective peaks in the spectra. The symbols $\bar{\Gamma}$ and $\bar{M}$ are symmetric points in the $\sqrt{3}\times\sqrt{3}$ SBZ. The strongly upward-dispersive S_1^* band appears only near the $\bar{\Gamma}$ point of the $\sqrt{3}\times\sqrt{3}$ SBZ, like the S_1 band of the initial $\sqrt{3}\times\sqrt{3}$-Ag structure. Compared to the original S_1 band (Fig. 2), the bottom of S_1^* band is much lower below E_F, which implies that the S_1^* band is occupied by more electrons. The S_1' band has similar energy position and dispersion to the original S_1 band around $\bar{\Gamma}$ point. Because the dispersion of the S_1' and S_1^* bands obeys mainly the $\sqrt{3}\times\sqrt{3}$ symmetry, they are considered to be remnants of the S_1 band of the initial $\sqrt{3}\times\sqrt{3}$-Ag structure. The interpretation of the nature of the S_1' and S_1^* bands will be discussed in Sec. IV.

There are extra small peaks around the middle between the $\bar{\Gamma}$ and $\bar{M}$ points as shown in Fig. 7, which are not observed in Fig. 2. These features come from the weak peaks satisfying the $\sqrt{21}\times\sqrt{21}$ periodicity mentioned above.

C. XPS for the respective surfaces

We measured the Si $2p$ core-level emission in XPS at RT from the Si(111)-7×7 clean surface, the initial $\sqrt{3}\times\sqrt{3}$-Ag surface, the $\sqrt{3}\times\sqrt{3}$-Ag surface covered by about 0.1 ML of additional Au, and the $\sqrt{21}\times\sqrt{21}$-(Ag+Au) surface. The binding energies of the level were measured to be 98.75, 98.28, 98.42, and 98.45 eV, respectively. The peak positions were determined from the centers of the FWHM's of the emission peak (we could not resolve the spin-orbit splitting in the $2p$ level because of poor monochromaticity of the illuminating x ray, but the peak shifts could be determined with ± 0.05 eV accuracy by numerical fittings). We changed the input power for the x-ray tube to confirm no photovoltaic effect by x-ray irradiation. These data can be used to evaluate the band bendings in the surface space-charge layer as discussed in the next section because the energy of the photoelectrons from the Si $2p$ level is so high (higher than 1 keV) that they are bulk sensitive, almost free from surface chemical shifts. The escape depth of our photoelectrons is about 2 nm, estimated from a so-called universal curve of electron escape depth as a function of kinetic electron energy,[26] which is long enough to diminish the effect of surface chemical shifts, but short enough compared to the band bending that extends over 200 nm for the doping concentration in our Si crystal.

IV. DISCUSSION

A. Si(111)-$\sqrt{3}\times\sqrt{3}$-Ag surface

According to the first-principles calculations,[11,12] the S_1 state at the initial $\sqrt{3}\times\sqrt{3}$-Ag surface originates from an antibonding electronic state between Ag and Si atoms, so that it should locate above E_F to be empty. However, at the real surface as shown in Fig. 2, the S_1-state band is partially filled by electrons. Johansson *et al.*[16] attributed this partial filling to electron transfer from donor levels in bulk because their sample was a heavily doped n^+ crystal. However, even p-type wafers exhibited the S_1 band below E_F as shown in our present study. Where do the electrons in the S_1 band come from?

First, we estimate the charge (electron) concentration trapped in the S_1 band. By assuming the S_1 band in Fig. 2 to be parabolic, the effective mass m^* of electrons in this band can be estimated from a relation between energy ϵ and wave vector k, $\epsilon=\hbar^2k^2/2m^*$, where $\hbar$ is the Planck constant divided by 2π. From Fig. 2, when k is the Fermi wave vector $k_F=0.11$ Å^{-1}, the energy ϵ measured from the bottom of the band is $\epsilon=0.18$ eV. Then we get $m^*=0.25m_e$, where m_e is the free electron's rest mass. This value of m^* is comparable to that of the conduction electrons in bulk $m^*=0.33m_e$. Since the density of states in a unit volume of a two-dimensional free-electron system is given by a constant $D=m^*/\pi\hbar^2$, the charge density Q_{S_1} filling the S_1 band is $Q_{S_1}=-D\epsilon=-1.8\times10^{13}e/\mathrm{cm}^2$, where e is the elementary charge. This density corresponds to 0.07 electrons per $\sqrt{3}\times\sqrt{3}$ surface unit cell.

Next we estimate the excess charge (hole) concentration accumulated in the surface space-charge layer. The surface E_F of the Si(111)-7×7 structure is known to lie 0.63 eV above the valence-band maximum.[20] So, by considering Si $2p$ shifts in XPS mentioned in Sec. III (from 98.75 eV at the 7×7 surface to 98.28 eV at the $\sqrt{3}\times\sqrt{3}$-Ag surface), the surface E_F for the $\sqrt{3}\times\sqrt{3}$-Ag structure should be 0.16 eV

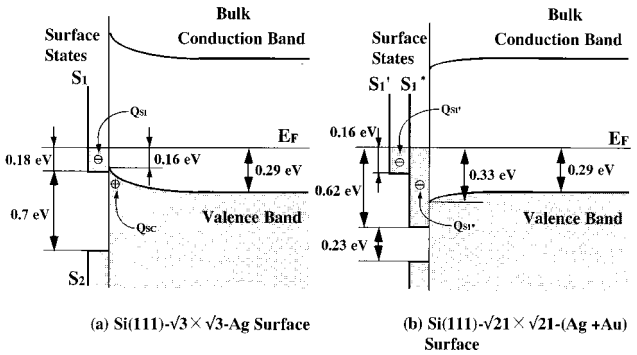

FIG. 8. Schematic illustrations of the surface states and the band bending in the surface space-charge layer at the (a) $\sqrt{3}\times\sqrt{3}$-Ag and (b) $\sqrt{21}\times\sqrt{21}$-(Ag+Au) surfaces, respectively. These are obtained from the results of ARUPS and XPS.

above the valence-band maximum. This E_F position is approximately the same as in previous reports.[16,21] On the other hand, for the Si wafer of p type used in this experiment, the distance between E_F and the valence-band maximum in deep bulk is 0.29 eV, estimated from the resistivity.[22,23] Therefore, the band bending in the surface space-charge layer is upward, as shown in Fig. 8(a). This means that the surface space-charge layer is a weakly hole-accumulation layer. Then the excess charge (hole) concentration Q_{SC} accumulated in the surface space-charge layer can be estimated. By solving the Poisson equation under the given band bending and integrating the accumulated hole concentration,[22] we can obtain $Q_{SC}=1.7\times10^{11}\ e/\mathrm{cm}^2$.

By comparing $-Q_{S_1}$ and Q_{SC} thus obtained, it can be said that the electron concentration trapped in the S_1 band is much larger than the hole concentration in the surface space-charge layer. So only a small number of the electrons in the S_1 band come from the substrate bulk (surface space-charge layer). However, the majority of them should come from other surface states (call S_X states), which are located above E_F. Such donor-type surface states are positively charged, whose (positive) charge concentration is Q_{S_X}, so that the neutrality is maintained: $Q_{SC}+Q_{S_X}+Q_{S_1}=0$, where $-Q_{S_1}\approx Q_{S_X}\gg Q_{SC}$. It is impossible at the present stage to answer a question whether these surface states S_X, which donate electrons into the S_1 band, are intrinsic or extrinsic (such as defect states). Experimentally, however, we can definitely say that the S_1 band is always partially filled by electrons, irrespectively of the doping type and doping concentration of Si wafers used and also of the surface preparation procedures. This suggests the nature of S_1-band filling to be intrinsic. On the other hand, we have found that a very small amount of Ag adatoms (less than 0.03 ML) deposited onto the $\sqrt{3}\times\sqrt{3}$-Ag surface donate electrons into the S_1 band.[24] This suggests another possibility that the electrons trapped in the S_1 band of the ''clean'' $\sqrt{3}\times\sqrt{3}$-Ag surface are extrinsically originated.

B. Si(111)-$\sqrt{21}\times\sqrt{21}$-(Ag+Au) surface

Compared to the initial $\sqrt{3}\times\sqrt{3}$-Ag surface, the Si $2p$ core level at the $\sqrt{3}\times\sqrt{3}$-Ag surface covered by 0.1 ML of Au shifted to higher binding energy by about 0.14 eV, as mentioned in Sec. III C. This means that the surface E_F lies 0.30 eV above the valence-band maximum on this surface. That is to say, the energy bands beneath the surface change into an almost flat-band condition because E_F in deep bulk lies 0.29 eV above the valence-band maximum. This indicates that the excess holes accumulated in the surface space-charge layer at the initial $\sqrt{3}\times\sqrt{3}$-Ag surface is depleted by adsorption of 0.1 ML of Au. However, compared to the initial $\sqrt{3}\times\sqrt{3}$-Ag surface in Fig. 1(a), the intensity of the S_1 peaks in the spectra was strengthened, as shown in Fig. 3, and its bottom was shifted down from E_F, as shown by open circles in Fig. 2. This means that the S_1 band is occupied by more electrons than at the initial surface. These electrons do not come from the substrate bulk, but from the Au adatoms because the surface space-charge layer is neutral (flat bands). If electrons were transferred from the surface space-charge layer into the S_1 band, more holes should be accumulated in the space-charge layer to maintain the neutrality. However, there is actually no excess holes in the layer. So it can be said that the excess electrons in the S_1 band do not come from the surface space-charge layer, but that the Au adatoms donate electrons into the S_1-state band (and also partially into the surface space-charge layer to diminish the excess holes therein). The charge (electron) concentration trapped in the S_1 band of the 0.1-ML-Au adsorbed $\sqrt{3}\times\sqrt{3}$-Ag surface is estimated in the same way as mentioned in Sec. IV A to be $Q_{S_1}=-2.9\times10^{13}\ e/\mathrm{cm}^2$. Therefore, the increment of the concentration ΔQ_{S_1} compared to Q_{S_1} of the initial $\sqrt{3}\times\sqrt{3}$-Ag surface is $\Delta Q_{S_1}=-1.1\times10^{13}\ e/\mathrm{cm}^2$. Since this ΔQ_{S_1} is provided by Au adatoms of about 0.1 ML coverage, each Au adatom donates approximately 0.1–0.2 electrons. This donor-type action of Au adatoms is the same as Ag adatoms deposited onto the $\sqrt{3}\times\sqrt{3}$-Ag surface.[24]

When the surface structure was transformed from the $\sqrt{3}\times\sqrt{3}$-Ag surface to $\sqrt{21}\times\sqrt{21}$-(Ag+Au) by Au deposition of about 0.19 ML, the Si $2p$ core level shifted towards higher binding energy by 0.17 eV compared to the situation of the initial $\sqrt{3}\times\sqrt{3}$-Ag surface (see Sec. III C). This means that the surface E_F is located 0.33 eV above the valence-band maximum and the band bending in the surface space-charge layer is slightly downward, as shown in Fig. 8(b). This indicates that the excess holes accumulated in the surface space-charge layer below the initial $\sqrt{3}\times\sqrt{3}$-Ag structure [Fig. 8(a)] are completely depleted. Because the band bending is downward, the surface states of the $\sqrt{21}\times\sqrt{21}$ structure must be positively charged in the net or at least the negative net charge must be reduced compared to that of the initial $\sqrt{3}\times\sqrt{3}$-Ag surface. Therefore, we have to say that the adsorbed Au atoms become positive by donating electrons into the S_1' and S_1^* surface-state bands as well as into the surface space-charge layer to diminish the holes therein. In other words, the Au adatoms make surface states well above E_F empty.

By assuming the S_1' and S_1^* bands to be parabolic (though they seem to be slightly asymmetric around the $\bar{\Gamma}$ point as shown in Fig. 7), we get the effective mass of electrons in the respective bands $m^*_{S_1'}=0.22m_e$ and $m^*_{S_1^*}=0.29m_e$. Since the energies at the bottoms of the respective bands are 0.16 and 0.62 eV measured from E_F as shown in Fig. 7, the charge

(electron) concentrations trapped in the bands are then calculated to be $Q_{S_1'}=-1.5\times10^{13}\ e/\mathrm{cm}^2$ and $Q_{S_1^*}=-7.4\times10^{13}\ e/\mathrm{cm}^2$, respectively. Therefore, the increment of the total charge (electron) concentration in these bands with respect to that in the S_1 band at the initial $\sqrt{3}\times\sqrt{3}$-Ag surface is given by $\Delta Q_{S_1'+S_1^*}=Q_{S_1^*}+Q_{S_1^*}-Q_{S_1}=-7.1\times10^{13}\ e/\mathrm{cm}^2$. These extra electrons come from the Au adatoms of 0.19 ML coverage. This means that each Au adatom in the $\sqrt{21}\times\sqrt{21}$ structure donates about 0.5 electron, which is slightly larger than the above-mentioned case of 0.1-ML-Au adsorption without the $\sqrt{21}\times\sqrt{21}$ superstructure. The amount of charge transferred from Au adatoms thus depends on whether or not they make a periodic arrangement (a $\sqrt{21}\times\sqrt{21}$ superstructure).

The large amount of electrons accumulated in S_1^* and S_1' is the origin for the very high electrical conductance of this surface; the surface space-charge layer hardly contributes to the electrical conduction because it is a depletion layer as mentioned above.[7,15]

In our previous paper,[7] from preliminary UPS measurements, we made a guess on the charge transfer between the Au adatoms and the Si substrate, which was the opposite to the present conclusion; the electron doping into the surface-state bands from the Au adatoms should not occur. That wrong conclusion was caused by overlooking the charge transfer from the Au adatoms into the bulk (surface space-charge layer). We have arrived at the opposite conclusion in the present paper only after the quantitative estimations of the charge concentrations accumulated in the surface-state bands as well as in the surface space-charge layer, as discussed above. The electrons should be actually transferred from the Au adatoms not only into the surface-state bands, but also into the surface space-charge layer. As described above, more electrons are trapped in the surface states S_1' and S_1^* at the $\sqrt{21}\times\sqrt{21}$-(Ag+Au) surface compared to in the S_1 state at the initial $\sqrt{3}\times\sqrt{3}$-Ag surface. These excess electrons in the surface states cannot come from the substrate because the surface space-charge layer is nearly neutral (a slightly depleted layer) beneath the $\sqrt{21}\times\sqrt{21}$ structure. This quantitative discussion results from our finding of the suitable illumination angles of UV light in ARUPS experiments, which was essentially important to detect the S_1 surface-state band of the initial $\sqrt{3}\times\sqrt{3}$-Ag surface and the S_1' and S_1^* bands of the $\sqrt{21}\times\sqrt{21}$-(Ag+Au) surface (in fact, we could not find the S_1 band in UPS spectra in the previous paper.[7]) We would like to correct the guess in Ref. 7 about the electron transfer.

C. Atomic bonding in the $\sqrt{21}\times\sqrt{21}$-(Ag+Au) structure

We next discuss the interrelation between the energy band structure and the atomic arrangement of the $\sqrt{21}\times\sqrt{21}$-(Ag+Au) surface. For this superstructure, Nogami, Wan, and Lin[1] and Ichimiya, Nomura, and Horio[2] proposed different models for its atomic arrangement. However, they did not explain how the Au adatoms bond to the substrate surface. The $\sqrt{3}\times\sqrt{3}$-Ag surface has no dangling bonds to be a stable surface with a low surface energy.[11–13]

This $\sqrt{3}\times\sqrt{3}$ framework does not seem to be severely broken in the $\sqrt{21}\times\sqrt{21}$-(Ag+Au) structure, as Nogami, Wan, and Lin and Ichimiya, Nomura, and Horio assumed. This expectation is reasonable if we consider some experimental facts: (i) The $\sqrt{21}\times\sqrt{21}$-(Ag+Au) domains easily slide on the surface, leaving the $\sqrt{3}\times\sqrt{3}$-Ag substrate behind during STM observations,[2,25] suggesting that Au adatoms simply adsorb and move on top of the $\sqrt{3}\times\sqrt{3}$-Ag substrate surface; (ii) the $\sqrt{21}\times\sqrt{21}$ superstructures are commonly formed on the $\sqrt{3}\times\sqrt{3}$-Ag surface by Ag or Cu adsorption as well as Au and these three $\sqrt{21}\times\sqrt{21}$ superstructures look very similar in STM and UPS measurements;[15] (iii) Ag adatoms on top of the $\sqrt{3}\times\sqrt{3}$-Ag surface at RT are extremely mobile to make a two-dimensional adatom gas phase,[24] while the $\sqrt{21}\times\sqrt{21}$ superstructure is formed only by cooling the surface below 250 K to reduce the mobility of Ag adatoms.[3,6] From these considerations, we can say that Au adatoms do not make covalent bonds with the substrate atoms of the $\sqrt{3}\times\sqrt{3}$-Ag structure. Our results of photoemission spectroscopies furthermore indicate some charge transfer between the Au adatoms and the substrate. So the bonding between them is not a physical adsorption such as van der Waals bonding. It is also impossible to say as ionic bonding because metallic bands (S_1^* and S_1') are detected in UPS experiments. We thus think it an interesting question how the adatoms are bonded to the $\sqrt{3}\times\sqrt{3}$-Ag surface having no dangling bonds.

For the $\sqrt{21}\times\sqrt{21}$ surface, Nogami, Wan, and Lin report by STM observations that Au adatoms lie on the Ag-trimer centers of the $\sqrt{3}\times\sqrt{3}$-Ag framework.[1] However, Ichimiya, Nomura, and Horio assume that Au adatoms lie on the Si-trimer centers of the $\sqrt{3}\times\sqrt{3}$-Ag structure.[2] Recently, we have found by STM observations that Ag adatoms also sit on the Ag-trimer centers of the $\sqrt{3}\times\sqrt{3}$-Ag framework to make a $\sqrt{21}\times\sqrt{21}$ superstructure by additional Ag adsorption at low temperatures.[15] This $\sqrt{21}\times\sqrt{21}$-Ag surface showed very similar STM images as the $\sqrt{21}\times\sqrt{21}$-(Ag+Au) surface induced by Au adsorption at RT. So we prefer to conclude that Au adatoms sit on the Ag trimers (though we do not completely agree with the model of Nogami, Wan, and Lin because of the different saturation coverage of Au adatoms). As mentioned below, this expectation seems to be consistent with our photoemission results in the present study and to be helpful in solving the above question how Au adatoms bond with the surface.

Figure 9 is a structural model of a single domain of the $\sqrt{21}\times\sqrt{21}$-(Ag+Au) phase with the underlying $\sqrt{3}\times\sqrt{3}$-Ag surface proposed by Nogami, Wan, and Lin.[1] The topmost layer consists of Au adatoms. The distances between the nearest-neighboring adatoms are mainly $\sqrt{3}a_0$, where a_0 is the length of the 1×1 surface unit vector, while some of them are $2a_0$ or $\sqrt{7}a_0$. We consider that these arrangements of adatoms raise a characteristic dispersion of the S_1' and S_1^* bands that mainly obeys the $\sqrt{3}\times\sqrt{3}$ periodicity. As the first trial to understand the nature and the origin of the surface-state bands in the $\sqrt{21}\times\sqrt{21}$-(Ag+Au) phase, we would like to suggest that the S_1 state of the initial $\sqrt{3}\times\sqrt{3}$-Ag surface is modulated by getting the electrons from the Au adatoms to be the S_1^*- and S_1'-surface-state bands in the $\sqrt{21}\times\sqrt{21}$ phase. By considering that the local density of states of the S_1 state is known to have maxima at the centers of Ag trimers of the $\sqrt{3}\times\sqrt{3}$-Ag framework,[11,12] we guess the nature of

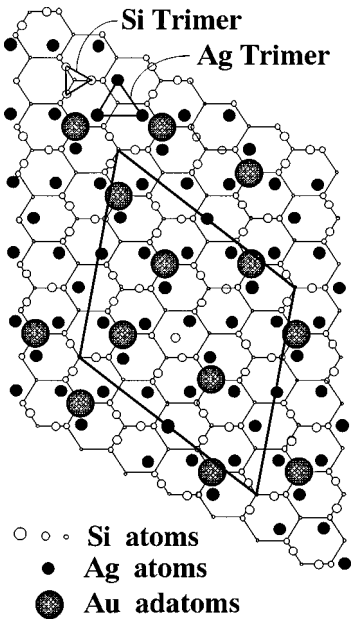

FIG. 9. Structural model of the $\sqrt{21}\times\sqrt{21}$-(Ag+Au) superstructure, made up of Au adatoms simply adsorbed on top of the $\sqrt{3}\times\sqrt{3}$-Ag framework, proposed by Nogami, Wan, and Lin (Ref. 1). The $\sqrt{21}\times\sqrt{21}$ unit cell is shown by a thick lozenge.

the S_1^* and S_1' states as follows. The surface state S_1^* originates from the Ag trimers on which the Au adatoms adsorb because the S_1^* state disperses mainly around the $\bar{\Gamma}$ point of the $\sqrt{3}\times\sqrt{3}$ SBZ and because they have additional photoemission of the $\sqrt{21}\times\sqrt{21}$ periodicity (as discussed with Figs. 4 and 5). The S_1' state, which also disperses around the $\bar{\Gamma}$ point of the $\sqrt{3}\times\sqrt{3}$ SBZ, is considered to come from the Ag trimers without Au adatoms. This is plausible if we consider that the number of ''bare'' Ag trimers is reduced at the $\sqrt{21}\times\sqrt{21}$-(Ag+Au) structure compared to at the initial $\sqrt{3}\times\sqrt{3}$-Ag surface, so that the intensity of the S_1' band becomes weaker at the $\sqrt{21}\times\sqrt{21}$-(Ag+Au) surface (Fig. 4) than that of the S_1 band in Fig. 1(a). However, of course, these guesses should be confirmed by further theoretical and experimental studies. In fact, the $\sqrt{21}\times\sqrt{21}$ phase has double domains rotating by 21.8° to each other, a halfway angle, which makes it very difficult to map the band dispersion in the single $\sqrt{21}\times\sqrt{21}$ SBZ. So, if we could prepare the $\sqrt{21}\times\sqrt{21}$ superstructure in single-orientation domains, a more detailed discussion would be possible.

Although there are no dangling bonds on the $\sqrt{3}\times\sqrt{3}$-Ag surface, there exists the S_1 band of an antibonding state. This surface state can trap electrons. According to our results of XPS, the electrons occupying the S_1^* and S_1' bands of the $\sqrt{21}\times\sqrt{21}$-(Ag+Au) surface come from Au adatoms sitting on the Ag trimers. This means that Au adatoms are positively ionized. Due to the Coulomb attraction between Au ions and the negative charge background in S_1' and S_1^* bands on Ag trimers, a stable surface structure will be formed. In addition, according to the model of the $\sqrt{21}\times\sqrt{21}$ structure (Fig. 9), every Ag trimer is not occupied by Au adatoms. The shortest distance between the nearest-neighboring Au adatoms is as small as $\sqrt{3}a_0$. So the electrons donated into the Ag trimers are not localized at the Au adatom sites, but they can travel into the neighboring Ag trimers that are without Au adatoms. This is plausible by considering the strong dispersions of the S_1' and S_1^* bands (as well as the original S_1 band), which means extended wave functions of these electronic states. In other words, Au adatoms can share electrons via these bands to form a two-dimensional metallic bonding among them. This may also be the origin of the high electrical conductance of the $\sqrt{21}\times\sqrt{21}$-(Ag+Au) phase.[7,8]

This is considered to be a different type of bonding for the surface superstructure on a semiconductor. Usual bonding on the surface is that the substrate atoms and the adatoms provide electrons simultaneously to form covalent bonds by sharing the two electrons and the resulting energy level splits into bonding and antibonding states. However, the $\sqrt{21}\times\sqrt{21}$ structure is a special case. The $\sqrt{3}\times\sqrt{3}$-Ag surface does not provide electrons for bonding, but only provides an antibonding surface state S_1. A bonding is formed between the adatoms and the surface via the surface state by energy resonance, resulting in a characteristic modulation in the energy level. Here we call this type of bonding parasitic surface bonding. This can be also the reason why Au adatoms sit on the Ag trimers instead of on the Si trimers. The Si trimers do not possess an antibonding state like the S_1 band. Therefore, the Au adatoms tend to sit on the Ag-trimer centers.

Then the Au adatoms are only loosely bonded with Ag trimers, compared to the case of usual covalent bondings. This is consistent with the following experimental facts: The $\sqrt{21}\times\sqrt{21}$ domains easily slide toward or against the tip depending on the bias-voltage polarity in STM observations[25] and the domains also show a ''waving'' behavior during STM observations.[2] These indicate that Au adatoms can easily migrate on the $\sqrt{3}\times\sqrt{3}$-Ag surface and also that the underlying $\sqrt{3}\times\sqrt{3}$-Ag framework is not severely destroyed by Au adsorption.

V. CONCLUSIONS

For the Si(111)-$\sqrt{21}\times\sqrt{21}$-(Ag+Au) structure, we have found two upward-dispersive surface-state bands S_1^* and S_1' crossing E_F. By estimating the charge concentrations in the respective surface-state bands and the surface space-charge layer, we conclude that Au adatoms donate electrons mainly into the S_1 band of an antibonding state at the initial $\sqrt{3}\times\sqrt{3}$-Ag surface. Then the electron wave function of the S_1 band is considered to be modulated to be the S_1^* band at Ag trimers on which Au adatoms sit and to be the S_1' band at Ag trimers without Au adatoms.

We proposed a kind of mechanism for atomic bonding in the $\sqrt{21}\times\sqrt{21}$-(Ag+Au) structure, referred to as parasitic surface bonding; adatoms make metallic bonds with each other via electrons accumulated in a surface-state band of the substrate.

The results in this experiment seem to support an atomic model of the $\sqrt{21}\times\sqrt{21}$-(Ag+Au) structure that Au adatoms adsorb atop the Ag trimers of the $\sqrt{3}\times\sqrt{3}$-Ag framework.

ACKNOWLEDGMENTS

We acknowledge Fumio Shimokoshi, Yuji Nakajima, Sakura Takeda, Tomohide Takami, and Tadaaki Nagao for

their experimental assistance and stimulating discussions. We also thank Professor Martin Henzler of Hannover University and Professor Shozo Ino of Utsunomiya University for their valuable discussions. This work has been supported in part by Grants-In-Aid from the Ministry of Education, Science, Culture, and Sports of Japan, especially through the New Frontier Program Grants-In-Aid for Science Research (Grants Nos. 08NP1201 and 09NP1201) and the International Scientific Research Program (Grant No. 07044133) conducted by Professor Katsumichi Yagi of Tokyo Institute of Technology. We have been supported also by Core Research for Evolutional Science and Technology of the Japan Science and Technology Corporation conducted by Professor Masakazu Aono of Osaka University and RIKEN.

---

*Present address: Semiconductors Laboratory, The Institute of Physical and Chemical Research (RIKEN), Wako, Saitama, 351-01, Japan.

†Present address: Surface and Interface Laboratory, The Institute of Physical and Chemical Research (RIKEN), Wako, Saitama, 351-01, Japan.

‡Author to whom correspondence should be addressed. Electronic address: shuji@surface.phys.s.u-tokyo.ac.jp

[1] J. Nogami, K. J. Wan, and X. F. Lin, Surf. Sci. **306**, 81 (1994).

[2] A. Ichimiya, H. Nomura, and Y. Horio, Surf. Rev. Lett. **1**, 1 (1994).

[3] Z. H. Zhang, S. Hasegawa, and S. Ino, Phys. Rev. B **52**, 10 760 (1995).

[4] I. Homma, Y. Tanishiro, and K. Yagi, in *The Structure of Surfaces III*, edited by S. Y. Tong, M. A. Van Hove, K. Takayanagi, and X. D. Xie (Springer, Berlin, 1991), p. 610.

[5] M. Lijadi, H. Iwashige, and A. Ichimiya, Surf. Sci. **357/358**, 51 (1996).

[6] X. Tong, S. Hasegawa, and S. Ino, Phys. Rev. B **55**, 1310 (1997).

[7] C.-S. Jiang, X. Tong, S. Hasegawa, and S. Ino, Surf. Sci. **376**, 69 (1997).

[8] S. Hasegawa, X. Tong, C.-S. Jiang, Y. Nakajima, and T. Nagao, Surf. Sci. **386**, 322 (1997).

[9] T. Takahashi and S. Nakatani, Surf. Sci. **283**, 17 (1993), and references therein; T. Takahashi, S. Nakatani, N. Okamoto, T. Ishikawa, and S. Kikuta, Jpn. J. Appl. Phys., Part 2 **27**, L753 (1988); Surf. Sci. **242**, 54 (1991); M. Katayama, R. S. Williams, M. Kato, E. Nomura, and M. Aono, Phys. Rev. Lett. **66**, 2762 (1991).

[10] S. Hasegawa and S. Ino, Int. J. Mod. Phys. B **7**, 3817 (1993); S. Hasegawa, Z. H. Zhang, C.-S. Jiang, and S. Ino, in *Nanostructures and Quantum Effects*, edited by H. Sakaki and H. Noge (Springer, Berlin, 1994), p. 330.

[11] S. Watanabe, M. Aono, and M. Tsukada, Phys. Rev. B **44**, 8330 (1991); Surf. Sci. **287/288**, 1036 (1993).

[12] Y. G. Ding, C. T. Chan, and K. M. Ho, Phys. Rev. Lett. **67**, 1454 (1991); **69**, 3817 (1993).

[13] T. Yokotsuka, S. Kono, S. Suzuki, and T. Sagawa, Surf. Sci. **127**, 35 (1983).

[14] S. Hasegawa, C.-S. Jiang, X. Tong, and Y. Nakajima, Adv. Colloid Interface Sci. **71/72**, 125 (1997).

[15] X. Tong, Y. Sugiura, T. Nagao, T. Takami, S. Takeda, S. Ino, and S. Hasegawa, Surf. Sci. (to be published).

[16] L. S. O. Johansson, E. Landemark, C. J. Karlsson, and R. I. G. Uhrberg, Phys. Rev. Lett. **63**, 2092 (1989); **69**, 2451 (1992).

[17] G. V. Hansson, R. Z. Bachrach, R. S. Bauer, and P. Chiaradia, Phys. Rev. Lett. **46**, 1033 (1981).

[18] S. Hasegawa, H. Daimon, and S. Ino, Surf. Sci. **186**, 138 (1987).

[19] T. Tsuno, Ph.D. thesis, University of Tokyo, 1990; S. Ino, in *Reflection High-Energy Electron Diffraction and Reflection Electron Imaging of Surfaces*, edited by P. K. Larson and P. J. Dobson (Plenum, New York, 1988), p. 7.

[20] F. J. Himpsel, G. Hollinger, and R. A. Pollack, Phys. Rev. B **28**, 7014 (1983).

[21] S. Kono, K. Higashiyama, T. Kinoshita, T. Miyahara, H. Kato, H. Ohsawa, Y. Enta, F. Maeda, and Y. Yaegashi, Phys. Rev. Lett. **58**, 1555 (1987).

[22] S. M. Sze, *Semiconductor Devices Physics and Technology* (Wiley, New York, 1985); D. R. Frankl, *Electrical Properties of Semiconductor Surfaces* (Pergamon, Oxford, 1967).

[23] C.-S. Jiang, S. Hasegawa, and S. Ino, Phys. Rev. B **54**, 10 389 (1996).

[24] Y. Nakajima, G. Uchida, T. Nagao, and S. Hasegawa, Phys. Rev. B **54**, 14 134 (1996); Y. Nakajima, S. Takeda, T. Nagao, S. Hasegawa, and X. Tong, *ibid.* **56**, 6782 (1997).

[25] T. Nakayama, D.-H. Huang, and M. Aono, Microelectron. Eng. **32**, 91 (1996).

[26] W. Mönch, *Semiconductor Surfaces and Interfaces*, 2nd ed. (Springer, Berlin, 1995), p. 9.